Supporting Information

Zhan et al. 10.1073/pnas.1018510108

SI Materials and Methods

Primary Mouse Embryonic Fibroblast (MEF) and Cerebellar Granule Neuron Precursor (CGNP) Cultures. Primary MEF cells were cultured from E13.5 to E15.5 embryos. Briefly, embryo trunks were dissected, trypsinized, and dissociated to single cells. MEF cells were cultured in DMEM media with 10% FBS. Primary CGNP cultures were derived from dissociated P4 mouse cerebella and cultured in DMEM/F12 media containing 25 mM KCl, N2, and 10% FBS. To induce Brg deletion, 4-OHT (1 μM) was added to *Brg$^{F/F}$; actin-CreER* MEF or CGNP cells for 2–3 d. For Shh stimulation, Shh conditioned media produced from Shh-CM 293T cells (1) were added 1:20 to MEF and CGNP cultures. MEF cells were treated with Shh in low serum media 24 h before harvesting. CGNP cells were treated with Shh in high serum media for 3 d. For drug treatment, trichostatin A (1 μM), cyclopamine (5 μM), or mouse bone morphogenetic protein 4 (50 ng/mL) was added to MEF cultures 24 h before harvesting.

Telencephalon Explant Culture. Telencephalons from E13 wild-type and *Brg*-mutant embryos were dissected and placed in culture media containing DMEM/F12 with putrescine, 2-mercaptoethanol, transferrin, insulin, selenium, progesterone, MEM vitamin additive, and 5% FBS. Cyclopamine (5 μM) or ethanol vehicle were added to the culture for 24 h and explants were harvested for RT-PCR analysis.

Induction of Brg Deletion in Vivo. To induce Brg deletion in developing cerebellum, P0 *Brg$^{F/F}$; Nestin-CreER* or control *Brg$^{F/F}$* pups were injected once s.c. with 50 μL of tamoxifen (6.67 mg/mL in sunflower oil). Mice were analyzed at postnatal day 9 (P9).

Plasmid Construction, Virus Preparation, and Transfection/Infection of MEF Cells. *Brg* shRNA in lentiviral vector pLKO1 (Openbiosystem; TRCN0000071384) was described previously (2). Lentiviral vector pSin4-EF2-IRES-Puro was used to generate expression constructs for Brg, BrgK785R, and tagged Gli full-length and truncated fragments. Lentiviruses were prepared according to a previously described procedure (3). PolyJet (Signagen) was used for plasmid transfection of cultured cells. MEF cells were infected in attachment at a multiplicity of infection (MOI) of 5 for 24 h in MEF media with 8 μg/mL polybrene.

Immunoblotting and Immunocytochemistry. For immunoblotting, cells or tissues were lysed in RIPA buffer (50 mM Tris pH 8, 250 mM NaCl, 0.05% SDS, 0.5% DOC, 1% NP-40) and cell lysates were separated on SDS/PAGE gels. Antibodies used were mouse monoclonal antibodies against Brg (G7; Santa Cruz Biotechnology), HSP90 (BD Pharmingen), Gli1 (Cell Signaling), β-catenin (E5; Santa Cruz Biotechnology), Nestin (BD Pharmingen), βIII-tubulin (Tuj1; Covance), HA (HA-7; Sigma), GFP (JL-8; Clontech), rabbit anti-Brg (H88; Santa Cruz Biotechnology), GAPDH (Sigma), HDAC1 (Abcam), HDAC2 (Invitrogen), Gli3 (kindly provided by Dr. Baolin Wang, Cornell University, Ithaca, NY), and goat anti-Gli3 antibody (R&D Systems). HRP-conjugated secondary antibodies were purchased from Jackson Immunology. Antibodies against acetylated tubulin (Sigma) were used to define primary cilia in 4-OHT or ethanol-treated *Brg$^{F/F}$, actin-CreER* MEF cells. Antibodies against Brg, Nestin, βIII-tubulin, and phosphorylated histone h3 (H3P-ser10; Upstate Biotechnology) were used for immunostaining of MEF cells or cultured CGNP cells.

Immunohistology and in Situ Hybridization. Timed mouse pregnancies were determined by plugging date as day 0.5. BrdU (100 μg/g) was injected 2 h before killing the mice. For immunohistology, paraffin sections were stained with antibodies against Olig2 (Chemicon), BrdU (Sigma), H3P (Upstate Biotechnology), and Ki67 (BD Pharmingen) and visualized using an Olympus BX50 microscope. BrdU$^+$ cells were counted from five random but comparable external granule layer (EGL) regions in control and *Brg*-mutant cerebella. EGL cells were judged by their DAPI staining location at the outer layer of cerebellum. A total of 2,000 EGL cells were counted in each mouse and the results were an average from three mice. For H3P$^+$ cells, a similar method was used for counting the cells. Ki67 was used as a proliferation marker and the majority of the EGL cells are Ki67$^+$.

Nkx6.2 in situ hybridization riboprobes (kindly provided by Dr. Jane Johnson, University of Texas Southwestern, Dallas, TX) were prepared from linearized templates using T7 RNA polymerase and DIG RNA labeling mix (Roche). Cryosections (20 μm) were hybridized with the riboprobes using protocols described earlier (4).

Coimmunoprecipitation Experiments. Affinity-purified antibodies used for immunoprecipitation (IP) were against Brg/Brm or the HA tag (rabbit; Abcam). J1 anti-Brg/Brm antibody has been well characterized and extensively used for affinity purification and proteomic studies of Brg/Brm associated factor (BAF) complexes (5–10). NIH 3T3 or HEK293T cells were transiently transfected with plasmids expressing HA-tagged full-length or truncated Gli proteins using PolyJet (Signagen). Mock transfection was used as negative control. Cells were harvested 48 h after transfection and were lysed with co-IP Lysis Buffer (50mM Tris pH8.0, 150mM NaCl, 1mM EDTA and 1% Triton X-100, with protease inhibitor freshly added). Cell lysates were snap frozen in liquid nitrogen and then thawed on ice followed by sonication to facilitate cell lysis. After centrifugation, appropriate antibodies were added to precleared cell lysate and incubated at 4 °C overnight. After incubating with protein A beads (GE Healthcare) for 1 h, beads were washed with co-IP buffer four times. Precipitated proteins were eluted by boiling in 2× sample buffer before SDS/PAGE and Western blot analysis. For detecting endogenous protein interaction, E13.5 telencephalon or P4 cerebellum were dissected and placed in co-IP lysis buffer. After homogenization, cell lysates were treated the same way as described above.

Bioinformatics Analysis. The genomewide binding sites of Brg and Gli3 were obtained from National Institutes of Health Geo Datasets database. All of the binding sites were assigned to annotated genes (n = 29,341) if they are in the gene body or within 5 kb upstream. The genes bound by both Gli3 and Brg and the genes containing overlapping Gli3/Brg binding regions were counted. Hypergeometric tests were used to calculate the P value for statistical significance.

Chromatin Immunoprecipitation (ChIP). ChIP experiments were performed using E13.5 mouse telencephalons or MEF cells. Dissociated tissues or cells were double crosslinked with disuccinimidyl glutarate (Pierce) and paraformaldehyde and sonicated to fragments (200–1,000 bp) (Fig. S5*C*). For immunoprecipitation, antibodies used were against Brg/Brm (J1), HDAC2 (Invitrogen), HA (Abcam), or acetylated H4 (mixed rabbit polyclonal antibody against histone 4 acetylated at lysine 5, 8, 12, or 16) (11). Rabbit

IgG was used as a negative control. Precipitated DNA was purified and subjected to real-time PCR. ChIP fold of enrichment was calculated using a fragment in CD4 gene as negative DNA control and IgG as antibody control.

RT-PCR and q-PCR. RNAs from cells or tissues were extracted with Trizol (Invitrogen) or the RNeasy kit (Qiagen). cDNAs were synthesized by reverse transcription using SuperScript III (Invitrogen), followed by PCR or quantitative PCR analysis. An ABI-7500 real-time PCR system was used for quantitative PCR. Levels of *GAPDH* mRNA were used to normalize input RNA. Graphics shown are representative of experiments performed in triplicate. SEs were calculated according to a previously described method (12). Sequences of PCR-primers used are

ChIP primers	Sequence
Gli1ChIP_P1F	GAAACACTGACGTCTTCCAACG
Gli1ChIP_P1R	TCTCTTTGTCCGCGCCTCT
Gli1ChIP_P2F	TGTTTTGCTTTAATTTGTGCCTTC
Gli1ChIP_P2R	CCGTCCCAACTGCTTCTTCA
Gli1ChIP_P3F	GGCAGTATAGGGTCCCTCAAGG
Gli1ChIP_P3R	AACTTTTTCTCGCTGTTGCCA
Gli1ChIP_P4F	GCTCTTCCCGCTCACTTCC
Gli1ChIP_P4R	GGCAGTATAGGGTCCCTCAAGG
Gli1ChIP_P5F	CGTAACTGAGCTTTCCCCATGT
Gli1ChIP_P5R	CCTTCATGTTCCATAGGTCGC
Gli1ChIP_P6F	GTGCTAGGACGACCAGCAGAG
Gli1ChIP_P6R	TGCATTCACAGATCACTGAGGAC
Gli1ChIP_P7F	ACTCCTTGCACTTGTTAGGTCTCAT
Gli1ChIP_P7R	AGGCGGATTTCTGAGTTCGAG
ChIP-Ptch1F	GGACAGAGCATCTACCCTAAAAGA
ChIP_Ptch1R	TCAGTTCTTTAAGCTCCTGCACTA
ChIP_Nkx6.1F	AATTTTTATTTTTCGGCATAGCTG
ChIP_Nkx6.1R	ATGGTAAGAGGTCATCCTTATTGC
ChIP_Nkx6.2F	CGGCTCGGGAAGTTTGCG
ChIP_Nkx6.2R	GCCGCCCTTAGTATCCCTGC
ChIP-CD4F	CACCCTACGCTGACATAGTGGTTC
ChIP-CD4R	GCAAGATAGCTAAGCCAAACACATT

RT-PCR primers	Sequence
Ptch1F	GAAGCCACAGAAAACCCTGTC
Ptch1R	GCCGCAAGCCTTCTCTAGG
Gli1F	GGTCTCGGGGTCTCAAACTGC
Gli1R	CGGCTGACTGTGTAAGCAGAG
Gli3F	caaccacagcccttgctttgc
Gli3R	GGCCCACCCGAGCTATAGTTG
ShhF	AGGGTCGAGCAGTGGACATC
ShhR	ATTTGGCCGCCACGGAGTT
Oligo2F	TTACAGACCGAGCCAACACCA
Oligo2R	GGGACGATGGGCGACTAGA
GapdhF	GTGGTGAAGCAGGCATCTGA
GapdhR	GCCATGTAGGCCATGAGGTC
HhipF	gttcaacctgcccagccactg
HhipR	ATGACGGCACGCTGGCTCA
Mash1F	TCTTAGCCCAGAGGAACAAGAG
Mash1R	GGCTGTCTGGTTTGTTTGTTTC
Gsh2F	CATGTCGGACCCACGGAGATTCCACTG
Gsh2R	GTGCTTCACGCGACGGTTCTGAAAC
Nkx62F	ggcatgaccgagagccaagtg
Nkx62R	GGCCGGTTGTATTCGTCATCGT
Gli2F	AGCTCCACACACCCGCAACA
Gli2R	TGCAGCTGGCTCAGCATCGT
Gli1RT5UTRf	gctggaggtctgcgtggtagag
Gli1RT5UTRr	GAGGAGGAGGAGGAAAGAGAGATCC
HAhuGli1F	ccatacgatgttccagattacgct
HAhuGli1R	ATGAGGTTAGCTTGGTGGCAGA
PkaF	catcgaccagcagggctatattcag
PkaR	CAGCCATCTCGTAGATGAGGACTCC
SmoF	CGCCAAGGCCTTCTCTAAGCG
SmoR	ATGCTGAGCCCAGGCAGAGG
SufuF	ATGGCCGGCACTTCACCTACAAG
SufuR	GGCCAGCTGTACTCTTTGGGAAG
NmycF	GTCTTCCCCTTCCCGGTGAAC
NmycR	CAAGGTATCCTCTCCGGAGGTGC
Id1F	ACAGCGGGCGAGGTGGTACT
Id1R	TTTGCGGTTCTGGGGCAGGG
Ccnd1F	AGACCTGTGCGCCCTCCGTA
Ccnd1R	CAGCTGCAGGCGGCTCTTCT
Math1F	CGCCACAGCCACCTGCTACC
Math1R	GAGGCACCCAGCTCGGGAGA

1. Chen JK, Taipale J, Young KE, Maiti T, Beachy PA (2002) Small molecule modulation of Smoothened activity. *Proc Natl Acad Sci USA* 99:14071–14076.
2. Ho L, et al. (2009) An embryonic stem cell chromatin remodeling complex, esBAF, is essential for embryonic stem cell self-renewal and pluripotency. *Proc Natl Acad Sci USA* 106:5181–5186.
3. Tiscornia G, Singer O, Verma IM (2006) Production and purification of lentiviral vectors. *Nat Protoc* 1:241–245.
4. Stankunas K, et al. (2008) Endocardial Brg1 represses ADAMTS1 to maintain the microenvironment for myocardial morphogenesis. *Dev Cell* 14:298–311.
5. Ho L, et al. (2009) An embryonic stem cell chromatin remodeling complex, esBAF, is an essential component of the core pluripotency transcriptional network. *Proc Natl Acad Sci USA* 106:5187–5191.
6. Khavari PA, Peterson CL, Tamkun JW, Mendel DB, Crabtree GR (1993) BRG1 contains a conserved domain of the SWI2/SNF2 family necessary for normal mitotic growth and transcription. *Nature* 366:170–174.
7. Lessard J, et al. (2007) An essential switch in subunit composition of a chromatin remodeling complex during neural development. *Neuron* 55:201–215.
8. Wang W, et al. (1996) Purification and biochemical heterogeneity of the mammalian SWI-SNF complex. *EMBO J* 15:5370–5382.
9. Wang W, et al. (1996) Diversity and specialization of mammalian SWI/SNF complexes. *Genes Dev* 10:2117–2130.
10. Zhao K, et al. (1998) Rapid and phosphoinositol-dependent binding of the SWI/SNF-like BAF complex to chromatin after T lymphocyte receptor signaling. *Cell* 95: 625–636.
11. Wan M, Zhao K, Lee SS, Francke U (2001) MECP2 truncating mutations cause histone H4 hyperacetylation in Rett syndrome. *Hum Mol Genet* 10:1085–1092.
12. Livak KJ, Schmittgen TD (2001) Analysis of relative gene expression data using real-time quantitative PCR and the 2(-Delta Delta C(T)) Method. *Methods* 25: 402–408.
13. Hui CC, Joyner AL (1993) A mouse model of greig cephalopolysyndactyly syndrome: The extra-toesJ mutation contains an intragenic deletion of the Gli3 gene. *Nat Genet* 3:241–246.
14. Bultman S, et al. (2000) A Brg1 null mutation in the mouse reveals functional differences among mammalian SWI/SNF complexes. *Mol Cell* 6:1287–1295.
15. Vokes SA, Ji H, Wong WH, McMahon AP (2008) A genome-scale analysis of the cis-regulatory circuitry underlying sonic hedgehog-mediated patterning of the mammalian limb. *Genes Dev* 22:2651–2663.
16. Vokes SA, et al. (2007) Genomic characterization of Gli-activator targets in sonic hedgehog-mediated neural patterning. *Development* 134:1977–1989.
17. Lee EY, et al. (2010) Hedgehog pathway-regulated gene networks in cerebellum development and tumorigenesis. *Proc Natl Acad Sci USA* 107:9736–9741.

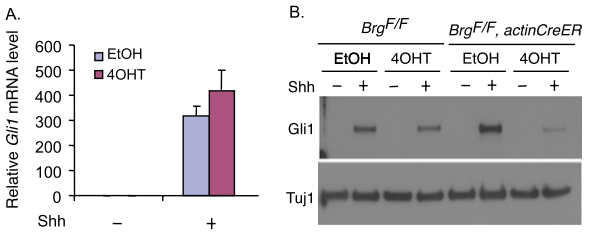

Fig. S1. 4-OHT has no significant effect on Shh target gene expression in MEF and CGNP cells. (*A*) qRT-PCR analysis of *Gli1* expression in $Brg^{F/F}$ MEF cells treated with 4-OHT or ethanol solvent in the absence or presence of Shh. (*B*) Western blot analysis of Gli1 expression in $Brg^{F/F}$ or $Brg^{F/F}$, *actin-CreER* CGNP cultures treated with 4-OHT or ethanol in the absence or presence of Shh.

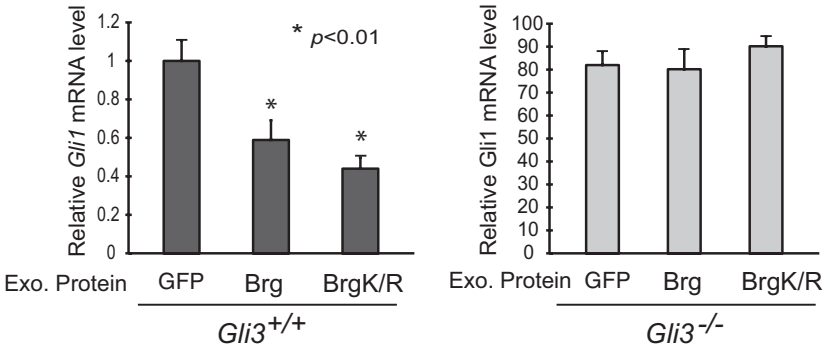

Fig. S2. Gli3 is required for Brg repressor function. Wild-type and $Gli3^{-/-}$ MEF cells were infected with lentivirus expressing GFP control, Brg, or BrgK785R protein. Relative *Gli1* mRNA levels were measured by qRT-PCR.

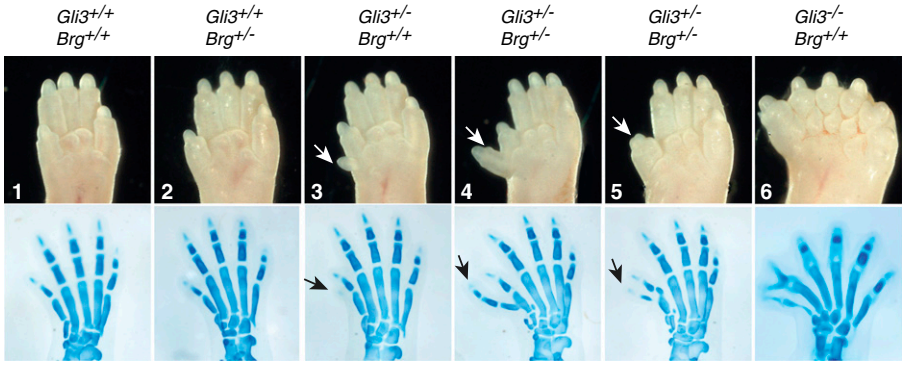

B.

	Hindlimb				Forelimb	
	Syndactyly	long extra toe	short extra toe	χ^2 test	extra 2nd toe	χ^2 test
Brg+/- (30)	0	0	0		0	
Gli3+/- (29)	0	0	29		1	
Gli3+/-, Brg+/- (34)	26	3	5	$p<<0.001$	7	$p<0.05$

Fig. S3. Genetic interaction between *Brg* and *Gli3* in regulating digit development. (*A*) Ventral view of hind limbs of E15.5 embryos with indicated genotypes. The first digits are on the *Left*. The alcian blue staining of limb skeleton with corresponding genotypes is shown below. $Gli3^{-/-}$ mice exhibit a polydactyly phenotype (panel 6) due to derepression of Shh target genes in developing limbs (13). $Gli3^{+/-}$ mice ($Gli3^{extra\ toe}$) usually have a preaxial extra toe or a small outgrowth (panel 3) due to haploinsufficiency (13). Although $Brg^{+/-}$ mice had no digit growth defects (panel 2) (14), double heterozygous mutations of *Gli3* and *Brg* led to an enhanced abnormal digit phenotype compared with *Gli3* single heterozygotes (panels 4 and 5). $Gli3^{+/-}$, $Brg^{+/-}$ mice often grew a preaxial extra toe longer than the first toe (panel 4) or had a fused first toe (syndactyly) (panel 5). (*B*) Quantifications of digit phenotypes of *Brg* and *Gli3* single and double heterozygotes. The significantly enhanced digit phenotypes observed in $Gli3^{+/-}$, $Brg^{+/-}$ double heterozygotes compared with $Gli3^{+/-}$ (χ^2 test, $P < <0.001$ for the hindlimb phenotypes, $P < 0.05$ for the forelimb phenotypes) suggest a genetic interaction between *Gli3* and *Brg* in repressing Shh target genes.

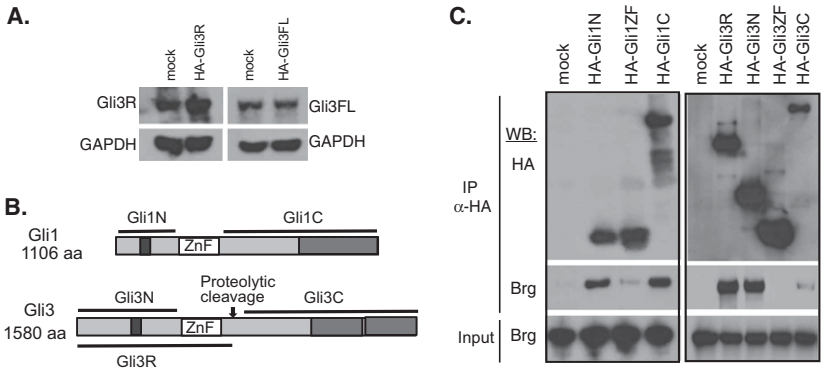

Fig. S4. Brg interacts with multiple regions in Gli transcription factors. (*A*) Western blot analyses of total Gli3 proteins using goat anti-Gli3 antibody in NIH 3T3 cells transiently transfected with plasmids expressing HA-Gli3R or HA-Gli3FL proteins (48 h). (*B*) A schematic drawing of the domain structures of Gli proteins and truncated mutants used in the study. (*C*) Both N-terminal and C-terminal regions of Gli proteins are sufficient to interact with endogenous Brg. Cell lysates of HEK293T cells transiently transfected with plasmids expressing HA-tagged Gli fragments (N-terminal, C-terminal regions, and Zn fingers of Gli1 and Gli3 proteins) were immunoprecipitated with anti-HA antibodies and blotted with antibodies against HA and Brg.

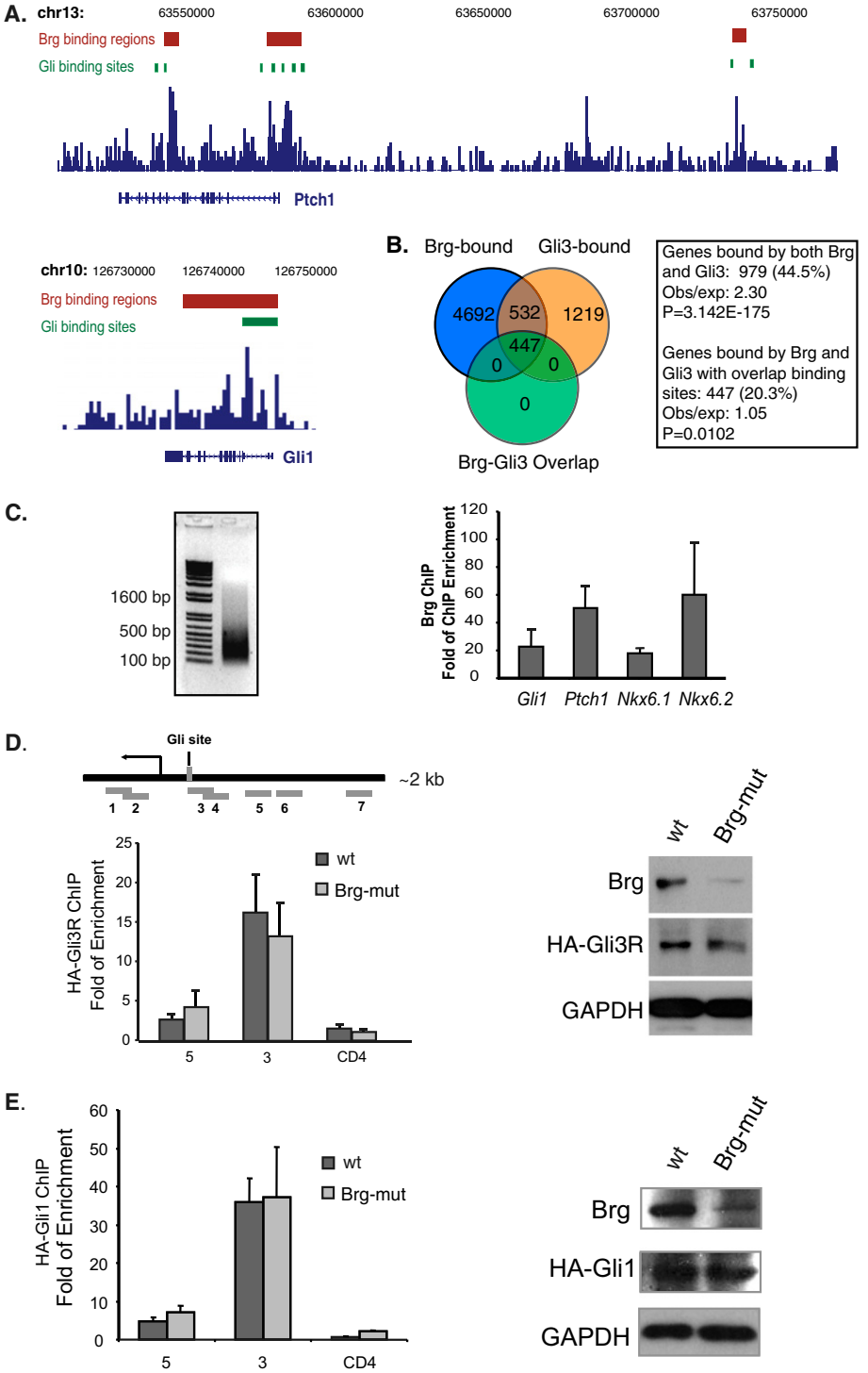

Fig. S5. Brg and Gli3 co-occupy Gli binding sites. (*A*) Comparison of Brg binding regions (red bars) (5) and Gli3 binding sites (green blocks) (15–17) around the mouse *Gli1* (~10 kb) and *Ptch1* genes (~200 kb). The blue peaks show the densities of Brg ChIP-seq sequencing tags (5). The location and the exon–intron structure of the genes are shown below the ChIP data. (*B*) Global comparison of genomewide Brg [embryonic stem (ES) cell] (5) and Gli3R (limb) (15) binding sites. Within the 2,198 genes bound by Gli3R, 979 (44.5%) genes contain Brg binding regions, in which 447 (45.7%) genes contain overlap Brg and Gli3 binding sites. Both are significantly higher than expected. (*C*) Brg binds to the Gli binding sites of Shh target genes. ChIP assays of E12.5 mouse telencephalons were carried out using the anti-Brg antibodies; rabbit IgG was used as a negative control. Primers were designed so that the PCR products were either near to or overlapping with the previously identified Gli binding sites (15–17). Sonicated DNA fragments are shown on the *Left*. (*D*) Gli3R binding to *Gli1* regulatory regions is not affected by Brg deletion. Wild-type and *Brg*-mutant MEF cells were infected with lentivirus expressing HA-Gli3R. Antibodies against HA tag were used for ChIP experiments. qPCR analysis of ChIP DNA is shown. A region in the *CD4* gene was used as a negative binding control. Expression of HA-Gli3R proteins in wild-type and *Brg*-mutant MEF cells is shown as Western blot. (*E*) Gli1 binding to *Gli1* regulatory regions is not affected by Brg deletion. Wild-type and *Brg*-mutant MEF cells were infected with lentivirus expressing HA-Gli1. Antibodies against HA tag were used for ChIP experiments. qPCR analysis of ChIP DNA is shown. A region in the *CD4* gene was used as a negative binding control. Expression of HA-Gli1 proteins in wild-type and *Brg*-mutant MEF cells is shown as Western blot.

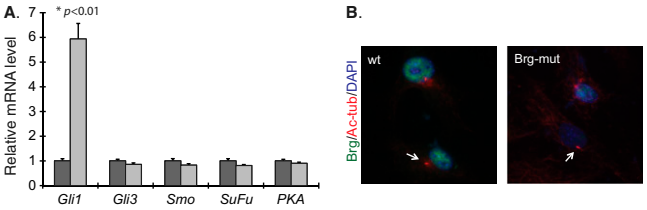

Fig. S6. Major components of Shh pathway are not affected by Brg deletion. (*A*) Levels of major components of Shh pathway genes in wild-type and *Brg*-mutant MEF cells were determined by qRT-PCR. (*B*) Primary cilia were formed in *Brg*-mutant MEF cells. Wild-type and *Brg*-mutant MEF cells were stained with antibodies against Brg (green) or acetylated tubulin (red). Primary cilia positive for acetylated tubulin are indicated by arrows.

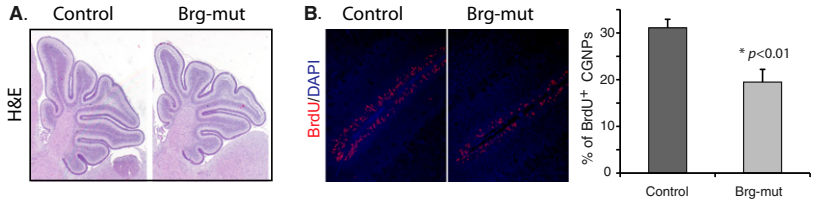

Fig. S7. Brg deletion in developing cerebellum leads to defective CGNP proliferation. (*A*) Hematoxylin and eosin staining of sagittal sections of P9 control and *Brg*-mutant cerebellum. *Brg*-mutant cerebellum is slightly smaller than the control cerebellum. (*B*) BrdU staining of P9 control and *Brg*-mutant cerebellum (2-h pulse). Comparable EGL regions are shown. Percentages of $BrdU^+$ cells in EGL regions were calculated and shown on the *Right* (2,000 cells per mouse counted, $n = 3$).

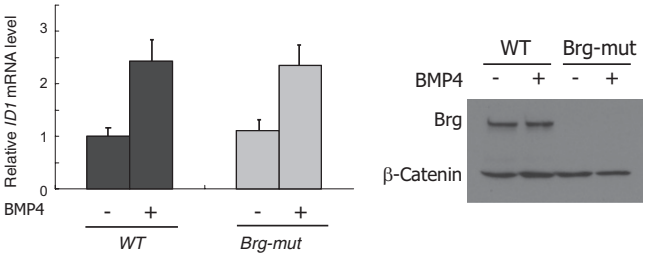

Fig. S8. Brg is not required for BMP4 regulated target gene expression. Wild-type or *Brg*-mutant MEF cultures were treated with BMP4 (50 ng/mL) for 24 h. Expression levels of BMP4 target gene *ID1* were measured by qRT-PCR. No significant differences on BMP4-induced *ID1* expression were observed between wild-type and *Brg*-mutant cultures.